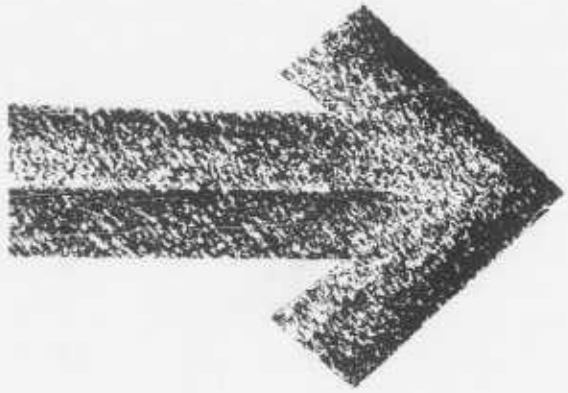

NMI-9522
Report Number

$4.60

United States Atomic Energy Commission
Division of Technical Information

OTI-131(May 1962)

USAEC Division of Technical Information Extension, Oak Ridge, Tennessee

NMI-9522

BERYLLIUM RESEARCH AND DEVELOPMENT PROGRAM

Quarterly Progress Report to
Aeronautical Systems Division

for the Period

April 1, 1962 through June 30, 1962

S. H. Gelles

November 5, 1962

Nuclear Metals, Inc.
Concord, Massachusetts

Contract No. AF33(616)-7065
Task Nos. 73518 and 735104

This report has been reviewed
and is approved

A. R. Kaufmann
Technical Director

TABLE OF CONTENTS

LIST OF TABLES

LIST OF FIGURES

LIST OF FIGURES

LIST OF FIGURES

I INTRODUCTION

This report describes the progress made on the Beryllium Research and Development Program for the period April 1, 1962, through June 30, 1962. Progress for the previous periods is summarized in the final report covering the work accomplished from April 1, 1960 through September 30, 1961, ASD-TDR-62-509 (NMI-9516, in press) and in the Quarterly Reports NMI-9517 and NMI-9519. The object of this program is to make beryllium more useful as an Air Force structural material.

The following is a list of the projects for the continued program and sites at which they are being carried out.

A Study of the Brittle Behavior of Beryllium by means of Transmission Electron Microscopy	Franklin Institute	F. Wilhelm H. G. F. Wilsdorf
Metallurgical Factors Affecting the Ductile-Brittle Transition in Beryllium	Lockheed Missiles and Space Company	M. I. Jacobson E. C. Burke
Preparation of Ultra-Fine Beryllium Powder	National Research Corporation	P. L. Raymond P. J. Clough
Preparation and Evaluation of Fine-Grained Beryllium	New England Materials Laboratory	A. S. Bufferd R. Widmer N. J. Grant
Recrystallization and Grain Growth in Beryllium	Pechiney Company	A. Saulnier R. Syre P. Vachet
Identification of Impurities and Precipitates in Beryllium	Pechiney Company	A. Saulnier R. Syre P. Vachet
Preparation and Evaluation of High-Purity Beryllium	Nuclear Metals, Inc.	E. Levine J. P. Pemsler
Fabrication and Evaluation of Fine-Grained Beryllium Produced from Ultra-Fine Powders	Nuclear Metals, Inc.	A. K. Wolff

During this report period, visits were made to the National Research Corporation and to The Franklin Institute to review the programs being carried out at each of these sites. In addition, personnel from New England Materials Laboratory visited Nuclear Metals, Inc. to discuss the program on the preparation and evaluation of fine-grained beryllium.

All the subcontracts have been signed and approved by the Air Force and work is under way at all of the subcontractor sites.

II. PROGRESS AT SUBCONTRACTOR SITES

A. Subcontract No. 4 - The Franklin Institute - F. Wilhelm and H. G. F. Wilsdorf - A Study of the Brittle Behavior of Beryllium by Means of Transmission Electron Microscopy

1. Precipitates in Commercially Pure Beryllium

It was reported earlier that numerous fine dark dots with diameters between 50 and 400 Å were discovered in beryllium crystals of commercial purity, when studied in the electron microscope. These dots were tentatively interpreted as precipitates for the following reasons:

a. The dots were never seen in the purer metal vacuum-melted from Pechiney flake nor in vacuum-distilled beryllium but consistently in commercial grade beryllium.

b. Dislocations seemed often to be pinned by these dark dots.*

c. Calculations of the critical shear stress, based on the theory of precipitation hardening, led to results that agreed fairly well with experimental values.

d. The appearance of the dark dots was not affected by washing the specimens in distilled water, alcohol, or treating them in weak acids or amonia.

- - - - - - - - - - -

*For an illustration, see Fig. 1 in "On the Behavior of Dislocations in Beryllium", presented at the Conference on the Metallurgy of Beryllium, October 1961, Institute of Metals, London, England.

However, after a variation in the electropolishing method for thinning down the electron transmission specimen was adopted[1], the little dots were no longer found.

After detailed studies of this phenomenon it must be concluded that the little dots are indeed a surface effect, created during the electropolishing process when an electrolyte was used of the composition:

100 parts H_3PO_4
30 parts H_2SO_4
30 parts glycerol
30 parts ethanol

It was possible to remove the dark dots from a specimen of commercial purity beryllium, which had been electropolished with the electrolyte mentioned above, by anodic etching in tartaric acid for 1/2 second, with a potential difference of 25 volts on the cell. Finally, it was possible to create an enhanced formation of the dark dots also on Pechiney flake beryllium, when an electrolyte of the above composition was used but which was aged for several months. Esterification and polymerization processes in the electrolyte may be responsible for the described artifacts. Since the observation of the dark spots was reported in the paper "On the Behaviour of Dislocations in Beryllium" at the London Conference on the Metallurgy of Beryllium in October, 1961, a corresponding correction has been made on the galley proofs.

It must be emphasized, however, that beryllium of commercial purity is not completely free of any foreign inclusions. Particles of 2μ diameter and smaller have occasionally been detected in thinned specimens, thus verifying observations of P. Vachet et al.[2] Figure 1 shows a series of particles with diameters ranging from 0.1 to 0.25μ, as seen in vacuum-melted and quenched beryllium (commercial purity).

2. Dislocation Studies

The study of a crystal of vacuum-distilled beryllium, obtained from NMI, which had been subjected to one "fast" zone-refining pass in the Metallurgy Laboratory at the Franklin Institute, has been completed. As previously stated[3] a tensile test specimen was machined

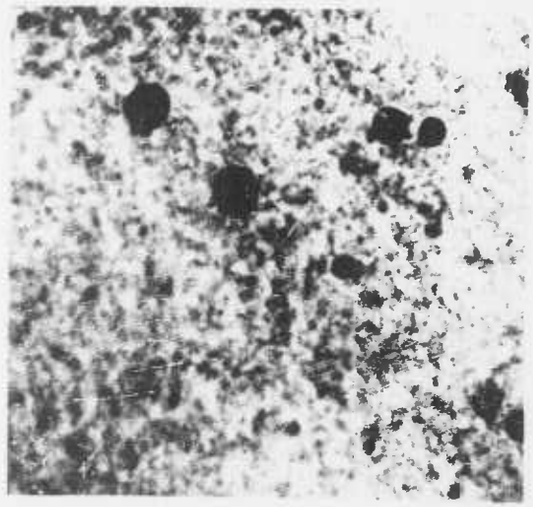

Fig. 1 - Inclusions in beryllium crystals of commercial purity. Diameters range from 0.1 to 0.25 μ.

from this crystal, the basal plane forming an angle of 45° with the tensile axis. The crystal was strained to fracture, and exhibited an elongation of 32.3 percent. Electron microscope specimens were cut from the crystal by electrolytic techniques so that the basal plane was viewed perpendicularly. Many dense bundles of dislocations were observed (see Fig. 3 of Reference 3) lying parallel to $(11\bar{2}0)$ planes. They are probably associated with the formation of "bend planes". The length of these bundles ranges from approximately 1 to 10μ, with an average length of 5μ. Their width is approximately 800 Å. About four bundles were counted within an area of 100 square microns. The dislocation density within the bundles is high. Assuming a thickness of 2500 Å for the specimens, the maximum observable dislocation density is calculated to be 10^{11} cm/cm^3. This density is exceeded within the bundles. Between the bundles typical dislocation densities range from 6 to 11 x 10^9 cm/cm^3 (Fig. 2). Using the formula $\gamma = \rho b \ell$, the average travel length ℓ for dislocations can be calculated. ρ is here the dislocation density, b the Burgers vector and γ the resolved shear strain. With the assumption of a specimen thickness of 2500 Å and a density of 10^{10} cm/cm^3 a dislocation travel length of 30μ is calculated.

Similarly high dislocation densities were obtained in specimens of commercial purity that were annealed at 1150°C for 1/2 hour and furnace cooled, then deformed by compression about 8%, with the basal plane forming an angle of 45° to the axis of compression and viewed in the direction of that axis. Figure 3 shows a typical micrograph of this series, with the dislocation density measured at 7 x 10^9 cm/cm^3. Many dislocations lying in zig-zag formation indicate a complex deformation mechanism; their 3-dimensional arrangement is yet to be determined. It will be necessary to study similar dislocation arrangements viewed perpendicularly to the prism planes in order to determine what glide systems are operative. Beryllium crystals of the proper orientation for this purpose have been requested from Nuclear Metals. Work is continuing on rapidly quenched single crystals of commercial purity (basal plane inclined

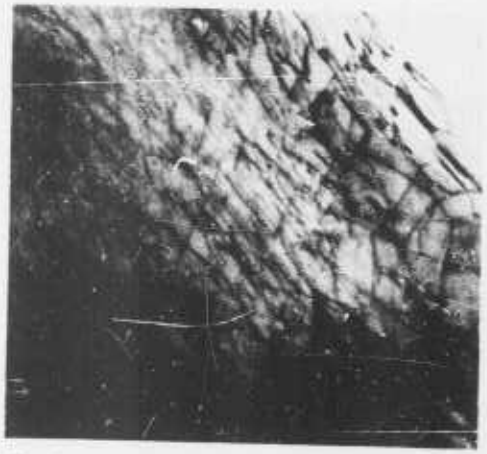

Fig. 2 - Dislocations in vacuum-distilled, zone refined single crystal beryllium, tensile-strained 32.3%. Principally one glide system is operative. Dislocation density 1.1 x 10^{10} cm/cm^3. 40,000X

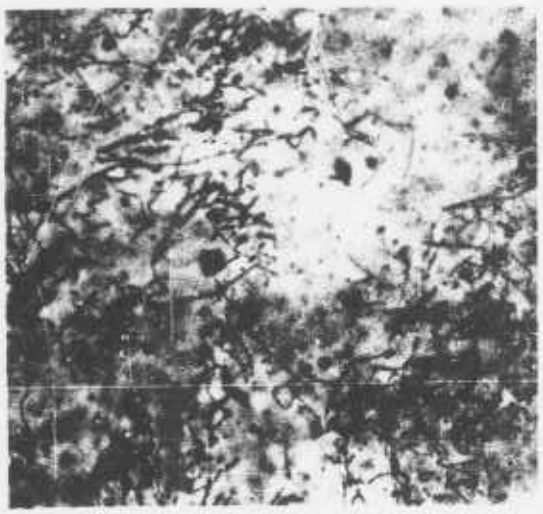

Fig. 3 - Dislocations of high density (ca 7 x 10^9 cm/cm^3) in compressed annealed beryllium single crystal of commercial purity. Deformation of the sample was 3%. 40,000X

45° to the axis of the specimen). Deformed and undeformed specimens are studied in order to investigate the possible influence of vacancies on the dislocation pattern.

B. Subcontract No. 5 - Lockheed Missiles and Space Company - M. I. Jacobson and E. C. Burke - Metallurgical Factors Affecting the Ductile-Brittle Transition in Beryllium

1. Introduction

The material necessary to conduct this investigation has been ordered and is expected to be available within the next two months. In the meantime, a review of the literature has been made with emphasis on the ductile-brittle transition theory in body-centered cubic metals and its applicability to beryllium. In particular, this report describes the theories of Stroh and Cottrell and indicates how the data obtained in the present study will be treated. A brief review of the factors influencing the ductile-brittle transition in beryllium is also presented.

2. Material Acquisition

Six pounds each of -60 +80, -150 +200, and -325 mesh nuclear grade powder have been ordered from Brush Beryllium for fabrication at Nuclear Metals. Delivery is expected early in July. There was some question as to whether the -60 +80 mesh powder would produce a dense ingot on hot pressing. Two pounds of this material were therefore sent to Nuclear Metals and a trial hot pressing made. The density of this pressing was determined to be 1.852 g/cc, which is close to theoretical, and metallographic examination showed no porosity.

An order was also placed with the Pechiney Company for 6 pounds each of -50 +120, -120 +200, and -200 +350 mesh CR grade powder. This is expected to be delivered to Nuclear Metals by the early part of August.

3. Theory of the Ductile-Brittle Transition

For beryllium, curves of tensile elongation vs. temperature generally show a sharp increase in elongation in the region 100-200°C. Because of the sharpness of the transition from cleavage fracture to ductile fracture, this may be regarded as being similar to the classical ductile-brittle transition in body-centered-cubic metals. However, the mechanism for the transition in beryllium may bear little or no relation to the transition in b.c.c. metals. The theories for b.c.c. metals are commonly based on a mechanism involving the stress concentration due to a dislocation pileup; hence, grain size and strain rate are significant variables. Since grain size and strain rate data will be available from the present investigation, a review of the theories pertaining to b.c.c. metals was made in the event that at least portions of the theories could be applied to the results of the present study. The theories of importance are those of Stroh and Cottrell, the essential points of which will be described briefly here. Petch's theory of the ductile-brittle transition was found to be inapplicable to beryllium.[8]

a. Theories of Stroh[4]

(1) Probability of Brittle Fracture. Stroh states that fracture occurs because there is no capacity for plastic flow, and that plastic flow may be prevented by the locking of dislocation sources. In b.c.c. metals, brittleness is apparently due to the Cottrell locking of dislocations. In h.c.p. metals, and in particular, beryllium, basal and prismatic slip are the primary deformation modes, with the critical resolved shear stress at room temperature for slip on the prism planes being about five times that for slip on the basal planes. This could mean that the Peierls stress on the prism planes is large and that dislocations would be unable to move without the aid of thermal fluctuations, or that the dislocations on the prism planes are locked by a Cottrell mechanism. Either of these would explain the decrease in critical resolved shear stress for the prism planes with increasing temperature.

Stroh assumes that if locked dislocations around a piled-up group can be freed by thermal fluctuations, the metal is ductile; however, if the temperature is too low to prevent a sufficient amount of thermal fluctuation, the stresses around a piled-up group become high enough to initiate a crack, and the metal is brittle. Therefore, the probability of brittle fracture is identified with the probability that the dislocations near a piled-up group will not be released.

The equation giving the probability that a locked dislocation will not be released by a stress-dependent activation energy, $U(\sigma)$, is given by Stroh as:

$$p = \exp[-\nu t \exp[-U(\sigma)/kT]] \qquad \text{(Eq. 1)}$$

where ν is a constant of dimensions of frequency, t is the time for which the stress on the dislocation is near the value σ, k is Boltzman's constant, and T is the absolute temperature. As a result of the double exponential, this function changes rapidly from 0 to 1 near a critical temperature, Tc, which is taken as the transition temperature. Because of this feature, the quantity p can take almost any positive value between 0 and 1, and is here assumed equal to 1/e. Therefore,

$$T_c = \frac{U(\sigma)}{k \ln \nu t} \qquad \text{(Eq. 2)}$$

In Eq. 2, the only factor depending on strain rate is t. Therefore,

$$t \propto \frac{\sigma}{\dot{\sigma}} \qquad \text{(Eq. 3)}$$

The stress, σ, which the piled-up group produces will increase in proportion to the applied stress, i.e., to $\sigma_f - \sigma_o$, which is that part of the applied stress σ_f which is not used in overcoming the frictional resistance to dislocation movement, σ_o. Hence,

$$t \propto \frac{\sigma_f - \sigma_o}{\dot{\sigma}_f} \qquad \text{(Eq. 4)}$$

However, according to Petch[5]

$$\sigma_f - \sigma_o = Kd^{-1/2} \qquad \text{(Eq. 5)}$$

where K is a constant and d is the grain diameter, so that

$$t \approx \frac{K}{\dot{\sigma}_f d^{1/2}} \qquad \text{(Eq. 6)}$$

If there is no yielding, $\sigma_f = E\epsilon$, so that $\dot{\sigma}_f = E\dot{\epsilon}$, and

$$t = \frac{K}{Ed^{1/2}\dot{\epsilon}} \qquad \text{(Eq. 7)}$$

If this is inserted into Eq. 2,

$$\frac{1}{T_c} = -\frac{k}{U(\sigma)} \ln \dot{\epsilon} + C \qquad \text{(Eq. 8)}$$

where

$$C = \frac{k}{U(\sigma)} \ln \frac{Ed^{1/2}}{k}$$

This gives a linear relation between $1/T_c$ and $\ln \dot{\epsilon}$ and the slope of the line provides an estimate of the activation energy $U(\sigma)$. It also indicates that transition temperature increases with strain rate, as is observed.

Grain size affects transition temperature in the following manner. It is assumed that as long as slip can occur in at least one grain, deformation can continue; however, if slip is halted in all grains, the stress at the head of a piled-up group of dislocations may be sufficient to nucleate a crack and cause brittle failure. The probability of a grain yielding at any time is the product of the number of grains considered and the probability $\nu \exp(-U/kt)$ of a given grain yielding. In a sample of uniform grain size, the number of grains in any region is proportional to d^{-3}; thus, ν can be redefined to include a factor proportional to d^{-3}. Since it was shown previously that $t \propto d^{-1/2}$, $\nu t \propto d^{-7/2}$. Again, if this is inserted into Eq. 4, the relation

$$\frac{1}{T_c} = -\frac{7}{2}\frac{k}{U(\sigma)} \ln d + C' \qquad \text{(Eq. 9)}$$

is obtained where C' is a constant that takes into account the unknown

proportionality constant. Equation 9 shows a linear relation between $1/T_c$ and $\ln d$, from which $U(\sigma)$ can be obtained. For steel, fairly good agreement was obtained between the activation energy obtained from Eqs. 8 and 9.

(2) Split Bend Plane Mechanism.[6] Beryllium has a single predominant slip plane, (0002), which is also the principal cleavage plane. According to Stroh, piled-up groups of dislocations produce no tensile stress normal to their own slip plane, and, hence, would not produce the kind of stress magnification needed for fracture. However, the $(11\bar{2}0)$ plane is a secondary cleavage plane in beryllium, and it is conceivable that pileups on the basal plane may cause sufficient stress magnifications normal to the $(11\bar{2}0)$ plane such that cleavage did occur on a $(11\bar{2}0)$ plane. Also, in a randomly oriented material, it is possible that basal pileups in one grain would be sufficient to cause basal fracture in an adjacent grain.

Stroh did, however, propose a mechanism whereby basal cleavage in a single crystal could be caused by a dislocation wall moving through the crystal, parallel to the slip plane. If part of the moving wall is held up at an obstacle, such as an impurity particle, the remaining part would continue to move under the applied stress, and cleavage of the slip plane would result. Cleavage could also occur on the slip plane according to a mechanism proposed by Gilman[7, discussion, p. 52] in which tensile stresses set up parallel to a non-moving tilt boundary are sufficient to cause cleavage.

Stroh recognized that grain boundary constraints would restrict the motion of a dislocation wall in a polycrystalline material, although it is the very presence of grain boundaries that make a pileup mechanism possible. He concluded that it might be possible to decide between a pileup and bend-plane mechanism by considering the variation of fracture strength σ_f with grain diameter d. The bend-plane model predicts an equation of the type

$$(\sigma_f - \sigma_o)\,\sigma_f = k/d \qquad \text{(Eq. 10)}$$

while the model based on dislocation pileups gives

$$(\sigma_f - \sigma_o)^2 = k/d \qquad \text{(Eq. 11)}$$

(3) Applicability of Stroh's Theories to the Current Investigation. The present study will produce data on the effects of grain size and strain rate on the transition temperature for beryllium of different purity, orientation, and heat treatment. For each of these materials, plots can be made of $1/T_c$ vs $\ln \dot{\epsilon}$ and $1/T_c$ vs $\ln d$, and the activation energies calculated. Previous work by Allen and Moore on vacuum cast and hot-worked electrolytic flake[8] indicated that linear plots would be obtained, although the activation energies determined from the two plots were different. In any event, it should be possible to obtain relative activation energies for each purity, orientation and heat treatment, so that the effective contribution of each of these variables to the brittleness problem can be determined.

Also, plots of σ_f vs $d^{-1/2}$ will permit a determination of k and σ_o, in Eqs. 10 and 11, so that Stroh's hypothesis regarding distinction between the bend-plane and pileup models may be tested.

b. Theory of Cottrell[9]

Cottrell's model for yielding is that dislocations pile up against the boundaries of yielded grains until the stress fields ahead of pileups are able to operate dislocation sources in adjacent unyielded grains. The equation for the applied stress at yielding, σ_y, is given as

$$\sigma_y = \frac{\sigma_i + \sigma_d (\ell/d)^{1/2}}{1 + (\ell/d)^{1/2}} \qquad \text{(Eq. 12)}$$

where σ_i is the lattice friction stress which opposes the motion of slip dislocations on their glide planes, σ_d is the stress required to unpin a dislocation from its atmosphere of impurity atoms, ℓ is the distance from the piled-up avalanche to the nearest source, and 2d is the grain diameter. Since ℓ is about 10^{-4} cm, for most grain sizes $d \gg \ell$,

and this equation simplifies to

$$\sigma_y = \sigma_i + k_y d^{-1/2} \qquad \text{(Eq. 13)}$$

where $k_y = \sigma_d \ell^{1/2}$.

Cottrell extends this model for yielding to include the case for brittle fracture by assuming that under certain circumstances some of the first dislocations to be generated on yielding coalesce to nucleate a crack. The crack may either propagate to cause fracture or be damped out by plastic deformation at its tip. The condition which must be satisfied if the crack is to propagate at the yield point is

$$(\sigma_i d^{1/2} + k_y) k_y \geq \beta \mu \gamma \qquad \text{(Eq. 14)}$$

or

$$\sigma_y k_y d^{1/2} \geq \beta \mu \gamma \qquad \text{(Eq. 15)}$$

where $\beta \simeq 1$ for tension, μ is the modulus of rigidity, and γ is the effective surface energy for fracture.

If, in Eq. 15, changes in $\beta \mu \gamma$ are assumed small enough to be neglected, then the effects of grain size, lattice friction stress, and strain rate on the transition temperature can be calculated. From Eq. 15

$$\frac{\partial(\sigma_y k_y d^{1/2})}{\partial T} \delta T + \frac{\partial(k_y \sigma_y d^{1/2})}{\partial d^{1/2}} \delta d^{1/2} = 0 \qquad \text{(Eq. 16)}$$

or

$$\frac{\delta T}{\delta d^{1/2}} = - \frac{\partial(\sigma_y k_y d^{1/2})/\partial d^{1/2}}{\partial(\sigma_y k_y d^{1/2})/\partial T} \qquad \text{(Eq. 17)}$$

If the differentiation is carried out, then

$$\frac{\delta T}{\delta d^{1/2}} = - \frac{k_y(\sigma_y + \frac{\partial \sigma_y}{\partial d^{1/2}} d^{1/2})}{d^{1/2}(\sigma_y \frac{\partial k_y}{\partial T} + k_y \frac{\partial \sigma_y}{\partial T})} \qquad \text{(Eq. 18)}$$

But,

$$\sigma_y = \sigma_i + k_y d^{-1/2}$$

so that $$\frac{\partial \sigma_y}{\partial d^{1/2}} = -\frac{k_y}{d}$$

which, by substitution, gives finally

$$\frac{\delta T}{\delta d^{1/2}} = -\frac{\sigma_i k_y d^{-1/2}}{\sigma_y \frac{\partial k_y}{\partial T} + k_y \frac{\partial \sigma_y}{\partial T}} \qquad \text{(Eq. 19)}$$

In the transition temperature region, values can be found for the parameters in Eq. 19 and a value of $\delta T/\delta d^{1/2}$ calculated. From this, the effects of changes in d on the transition temperature can be calculated. Cottrell showed that the results obtained for steel agreed with Eq. 19.

By similar arguments, equations can also be written for the effects of strain rate and lattice friction stress on transition temperature, namely

$$\frac{\delta T}{\delta \dot{\epsilon}} = -\frac{\partial (\sigma_y k_y)/\partial \dot{\epsilon}}{\partial (\sigma_y k_y)/\partial T} \qquad \text{(Eq. 20)}$$

$$\frac{\delta T}{\delta \sigma_i} = -\frac{\partial (\sigma_y k_y d^{1/2})/\partial \sigma_i}{\partial (\sigma_y k_y d^{1/2})/\partial T} \qquad \text{(Eq. 21)}$$

(1) Applicability of Cottrell's Theory to the Current Investigation. By plotting the data obtained in the present study in terms of σ_y vs $d^{-1/2}$ for each material and condition, the quantities σ_i and k_y can be determined. Also, the variation of k_y and σ_y with temperature and strain rate can be determined, which will permit estimates to be made of the effects of d, $\dot{\epsilon}$, and σ_i on transition temperature. The calculated values can then be compared with the observed values.

C. Consideration of the Pileup Mechanism

The theories of Petch and Cottrell are both based on a dislocation pileup mechanism, so a calculation of the cleavage stresses produced by such a pileup might be worthwhile.

The number of dislocations, n, which can be piled up in a length of slip line, L, between a source and a barrier under an applied shear stress σ_s is given by Eshelby, Frank, and Nabarro[10] as

$$n = \frac{L\sigma_s}{2A} \qquad \text{(Eq. 22)}$$

where $A = \mu b/2\pi(1-\nu)$ for edge dislocations and

μ = Shear modulus

b = Burgers vector

ν = Poisson's ratio

Koehler[11] calculated the tensile stress σ_T across a plane perpendicular to the slip plane containing the piled-up group and obtained

$$\sigma_T = \sim n\sigma_s \qquad \text{(Eq. 23)}$$

Therefore

$$\sigma_T = \frac{L\sigma_s^2}{2A} \qquad \text{(Eq. 24)}$$

If σ_T is greater than the theoretical cohesive strength, σ_M, fracture should occur. Thus, the criterion for fracture is

$$\frac{L\sigma_s^2}{2A} \geq \sigma_M \qquad \text{(Eq. 25)}$$

Since σ_M and A are constants, the shear stress σ_s necessary for fracture depends on the length L available for dislocation pileup, or on d, the grain diameter. Thus,

$$\sigma_s \propto \frac{1}{\sqrt{L}} \propto \frac{1}{\sqrt{d}}$$

a relationship which has been found to be true for beryllium.[8]

For beryllium, $\mu = 1.1 \times 10^{12}$ dyne/cm^2, $b = 2.3 \times 10^{-8}$ cm, and $\nu \sim 0.1$, so that

$$A = \frac{\mu b}{2\pi(1-\nu)} \simeq 4.5 \times 10^3 \text{ dyne/cm}$$

If we consider that the length available for dislocation pileup, L, is equal to d/2, and σ_s is equal to one-half the applied tensile stress,

then a calculation of the left hand side of Eq. 25 can be made from available data. Taking $d/2 = 8.5 \times 10^{-4}$ cm, and $\sigma_s = 1.7 \times 10^9$ dyne/cm^2 (Ref. 12, p. 163)

$$\frac{L\sigma_s^2}{2A} = \frac{8.5 \times 10^{-4} (1.7 \times 10^9)^2}{2 \times 4.5 \times 10^3} = 2.7 \times 10^{11} \text{ dyne/cm}^2$$

Other values of grain size and fracture stress give similar results.

A calculation of the theoretical strength of beryllium must now be made. According to the equation derived by Petch[13] the theoretical cleavage strength is

$$\sigma_M \sim \left(\frac{E\,S}{a}\right)^{1/2} \qquad \text{(Eq. 26)}$$

Where E is Young's modulus, S is the surface energy, and a is the lattice parameter. Since no value of S could be found, one was calculated according to the method of Zener and Hollomon[14] where $S = qN^{2/3}$. Here, N is the number of atoms/unit volume and q is the energy required to evaporate a single atom. The quantity q can be found from vapor pressure data as follows:

$$\frac{\eta q}{R} = \frac{d \ln P}{d\,1/T} \qquad \text{(Eq. 27)}$$

where η = Avogadro's number and R = 2 cal/g atom. Vapor pressure data for beryllium (Ref. 12, p. 311) give

$$\eta q = 37{,}000 \text{ cal/g atom}$$

from which

$$q = 6.12 \times 10^{-20} \text{ cal}$$

For beryllium, $N^{2/3} = 24.5 \times 10^{14}$/cm^2, so that $S = 6120$ ergs/cm^2.

The theoretical cleavage strength can now be determined, using $E = 3 \times 10^{12}$ dyne/cm^2, as

$$\sigma_M \sim \left(\frac{3 \times 10^{12} \times 6120}{2.3 \times 10^{-8}}\right)^{1/2} \simeq 9 \times 10^{11} \text{ dyne/cm}^2$$

Although this is slightly higher than 2.7×10^{11} dynes/cm^2, indicating that the pileup would not produce sufficient stress to cause cleavage, the agreement is not so bad that the pileup mechanism can be ruled out.

Moreover, the estimation of the theoretical cleavage strength may be somewhat high, since the calculated surface energy is higher than the values 1000-2000 ergs/cm^2 observed for many metals.

4. Previous Studies of Effects of Grain Size, Strain Rate, etc. on Ductile-Brittle Transition in Beryllium

A transition from ductile to brittle behavior at 200-300°C, in samples taken from the longitudinal direction of an extrusion, was first observed by Kaufmann, Gordon, and Lillie.[15] However, samples from the transverse direction showed no such transition. The increase in ductility between room temperature and 400°C was attributed to a decreasing tendency to develop fracture on (0001) planes, a decreasing ease of $\{10\bar{1}2\}$ twinning, and an increasing ease of slip on $\{10\bar{1}0\}$ planes as temperature increases (Ref. 12, p. 418). Martin and Ellis[16] cite two additional possibilities for the increase in ductility above room temperature:

(1) The onset of pyramidal slip, possibly in a direction that has a component along the "c" axis.

(2) An increasing ability for basal glide to occur without the formation of bend planes, as the temperature is raised, or to an increased ability for bend planes, once formed, to migrate under the influence of the applied stress.

The subject of the ductile-brittle transition in beryllium has recently been reviewed by Allen and Moore.[8] They concluded that the treatments used for b.c.c. metals could not be applied completely to beryllium because of the complicating effects of polygonization, and because of operation of the split bend plane mechanisms of Stroh and Gilman.

The more general problem of ductility in beryllium has been the subject of several recent papers[16-18] and there is little point in repeating the discussions here. However, it might be worthwhile to review briefly the experimental observations that are pertinent to the present investigation. The discussion will be confined to the effects of various factors on the tensile properties of beryllium below 400°C.

a. Effects of Grain Size

It is well established that material with fine grain size exhibits improved ductility, and that decreasing the grain size lowers the transition temperature.[16-21] Using the data of Bunce and Evans,[21] Allen and Moore[8] plotted $1/T_c$ vs ln d, according to Eq. 9, and obtained an activation energy of 11 kcal/mol.

b. Effects of Strain Rate

Increasing strain rate has been shown to decrease ductility and increase the transition temperature.[19,20,22] A calculation by Cotterill et al.[22] for cast and extruded electrolytic flake, according to Eq. 8, indicated an activation energy for flow of 47 kcal/mol. This is much higher than the 11 kcal/mol reported by Allen and Moore for rolled sheet, but the difference may be due to the difference in orientation between the sheet and the rod.

c. Effects of Purity and Thermal Treatment

The effects of purity and thermal treatment on the mechanical properties of polycrystalline beryllium are strongly related, but in cases where the purity of polycrystalline material was considered alone, the material with the higher purity exhibited the better ductility in the region from room temperature to 400°C.[20,21]

Thermal treatments, designed to improve the ductility of beryllium by precipitating solute elements, notably iron, from solution, markedly improve the ductility of beryllium above 400°C. Although some improvements have been noted as low as 200°C, such overaging treatments have been singularly unsuccessful in improving room temperature ductility.[21,23,25]

This is rather puzzling in view of the observation that the aging treatments result in the general precipitation of a supposedly iron-rich phase.[23] Wolff, Gelles, and Aronin[26] were able to improve the room temperature ductility of extruded rod that had been quenched from 1100°C and aged, but were unable to exceed the elongation of the as-extruded

rod. A possible explanation for the observation that overaging generally produces no increase in room temperature ductility is that, although the amount of iron in solution is reduced, softening the matrix, it precipitates in such a manner that a dispersion-hardened alloy is produced. This would tend to inhibit the ductility at low temperature.

d. Effects of Orientation

Extruded or rolled products have been shown to exhibit good tensile elongation in those orientations for which basal slip is inhibited. A particularly good example of the effect of orientation on the transition temperature is shown in the paper by Bunce and Evans.[21] Here, the transition temperature in the longitudinal direction (prism slip predominant) was some 200°C lower than in the transverse direction (basal slip predominant), and elongations at all temperatures were superior in the longitudinal direction.

It will be interesting to compare the results obtained in the present investigation on random and oriented material in terms of the activation energies for slip.

C. Subcontract No. 8 - National Research Corporation - P. L. Raymond and P. J. Clough - Preparation of Ultra-Fine Beryllium Powder

1. Introduction

The technique of producing high-strength materials by powder metallurgy methods has been employed for some time. The aim of this current program is to produce beryllium in ultra-fine powder form in order to determine if fine-grained powder metallurgy bodies of beryllium can be produced. If so, light-weight, high-strength components not currently available by other production techniques may be produced.

2. Evaporator Design and Construction

The design, construction and installation of the 4-foot diameter stainless steel vacuum evaporator has been completed, together with the dry-box assembly. At the present time the system is being vacuum tested.

Figure 4 shows the interior of the large mild steel tank with the various components of the beryllium production facility located inside. The evaporator tank is to the left. Glove ports on the front of the tank will permit manipulation within the system without having to open up to atmosphere. A large air-operated high vacuum valve separates the main evaporator tank from the dry-box. It is through this dry-box that the beryllium powder will be removed and the container washed down before it is removed from the system.

The evaporator consists of a 4-foot diameter by 4-foot high tank with a removable conical bottom 2 feet high. The removable bottom is to permit access to the internal components of the evaporator when necessary.

Within the evaporator chamber will be located the evaporation source, induction coil and power feedthrough, water-cooled powder collection drum and the container rack for receiving the powder from the drum. The evaporation chamber is also fitted with a 12 x 16-inch sight port and a pair of glove ports isolated from the working chamber by vacuum slide valves.

Attached to the evaporator chamber through a 12-inch air-operated vacuum valve is the stainless steel dry-box approximately 26 inches long by 18 inches high by 18 inches deep. This box is fitted with glove ports and slide valves as well as hinged access ports on the outermost end of the box.

The vacuum system consists of a 12-inch oil booster pump, a 200-c.f.m. rotary gas ballast mechanical pump, a 30-c.f.m. rotary gas ballast pump and a 6 c.f.m. backing pump. The 200-c.f.m. mechanical pump will be used to rough down the evaporator and will also be used to back the oil booster pump. The oil booster pump will handle 6000 c.f.m. in

Fig. 4 - View of the interior of mild steel tank showing evaporation and dry-box assembly for production of ultra-fine beryllium powder.

the 100- to 10-micron pressure range in the tank, which will be the operating range of the powder production program. The 6-c.f.m. holding pump will be used to back the booster pump when it is hot but not pumping on the system. The 30-c.f.m. pump will be used to evacuate the dry-box as needed.

Electrical wiring is now being installed and should be completed shortly. The main vacuum pump has been installed and the system is undergoing vacuum leak testing.

3. Air Ventilating System

The exhaust air system for the large tank will be installed during the first week of July. This system has been designed by Mr. Frederick Viles of Industrial Hygiene Associates. The air flow has been designed to permit 2000 cubic feet per minute to enter the top of the large tank through a filter. The air will exhaust through four flexible lines adjacent to each glove port and through a movable line which will be used to vent the inside of the evaporator when it is open for personnel to work inside.

The air will be discharged above the parapet of the roof of the building through a 12-inch pipe at a velocity in excess of 2500 feet per minute. The discharge of the fore (vacuum) pump will pass through a filter and then into the exhaust line where it will be discharged with the air from the large tank or clean room.

Two air sampling pumps and sampling assemblies will be used, one in the main working tank where the operating personnel will work and the other at the discharge of the exhaust fan on the roof. The sampling heads are standard dust sampling filter assemblies available from the Gelman Company.

4. Personnel Safety and Hygiene

Physical examinations and chest X-rays have been completed for four technicians and two engineers who will be working on the program. The medical records of these people have been reviewed by

Dr. Albert O. Seeler, who has indicated that none of the personnel who will work on the program has any pre-existing condition which would preclude his working with beryllium. It is planned that all those who will work in the "clean room" will be provided with coveralls which will be laundered commercially.

All personnel will be required to shower and change to street clothes before leaving the plant. Shoes will be wiped when leaving the tank. When the evaporator itself must be entered, the tank will first be brought to atmospheric pressure and then flushed well with a water spray manipulated through the glove ports before the tank is opened. Personnel entering will be required to wear hats, coveralls and respirators to prevent inhalation of airborne particles. The inside of the dry-box will be kept wet when it is open to prevent the incidence of beryllium dust. Once the program is under way, it is expected that personnel will be required to enter the evaporator only infrequently.

5. Planned Operation

It is expected that the powder production facility will be in operation in July as soon as the air ventilation system has been installed. Previous to that, however, it will be possible to operate and check out the system using aluminum as a source material. This will permit proper adjustment and location of the evaporation source and collection drum. It will also permit the technicians to become familiar with working in the system while transferring powder from the evaporator to the dry-box and with sealing the containers and washing them down. By working with aluminum the possibility of accidental exposure to toxic material is eliminated and the system can be more readily checked out.

When the powder production assembly is functioning as planned, the evaporator and dry-box will be washed down chemically to minimize aluminum contamination in subsequent beryllium runs. At that time, work will begin in investigating the series of variables of beryllium powder production outlined in the first quarterly report, namely,

evaporation rate, residual evaporation pressure and collection plate temperature and speed of rotation. It will then be possible to make experimental quantities of beryllium powder available to Nuclear Metals, Inc. for preliminary evaluation.

D. Subcontract No. 9 - New England Materials Laboratory - A. S. Bufferd, R. Widmer, and N. J. Grant - Preparation and Evaluation of Fine-Grained Beryllium

1. Introduction

The objective of this work is to prepare beryllium powder of very fine particle size, to evaluate the properties of fine-grained products prepared from this powder, and to determine the effect of oxide on these properties.

The mechanical properties of beryllium have been found to be highly dependent on grain size, which, in the powder metallurgy of beryllium, appears to control the oxide content, owing to the high affinity of beryllium for oxygen. Three general trends have been reported on: first, that the BeO layer present on powder particles stabilizes the grain size, so limiting grain growth; second, that the degree of preferred crystallographic orientation decreases with increasing BeO content, thus resulting in a more isotropic structure; and third, that the strength and ductility of beryllium increase with decreasing grain size.

2. Experimental Results

Minus 200 mesh QMV nuclear grade beryllium was ground in a methyl alcohol bath in a Szegvari attritor, 400 c.c capacity, manufactured by Union Process Co., Akron, Ohio. The attritor has a vertical spiked stainless steel shaft which rotates at a speed of 250-360 rpm. Stainless steel balls 3/16-inch diameter were used. The grinding charge was composed of 150 grams of powder, 150 ml of liquid and 1500 grams of stainless steel balls. Samples were taken every two hours for particle size and chemical analysis. The particle size was

determined by metallographic techniques, and chemical analyses for iron and oxygen content were conducted by Nuclear Metals*. The sample powders for oxygen analyses were cold compacted by either hydrostatic pressing or die pressing. The compacted specimens were then vacuum treated at 300°F to remove any residual volatiles from the grinding operations. The results of these measurements are summarized in Table I.

Although the desired particle size range was reached, the high iron and oxide contents are quite disturbing. To determine the source of iron contamination, chemical analysis for chromium was conducted (Table II), since the attritor components are 18-8 stainless steel.

The approximate 4:1 ratio between iron (see Table I) and chromium contents indicates the source of contamination to be the stainless steel components of the attritor. The analysis for oxygen after 12 hours grinding (10.8 percent BeO) may not be a representative value, for the powder had been stored in the dry-box for approximately three weeks prior to cold compacting.

Since the grinding medium is an alcohol, the carbon content of dried but not vacuum treated, powder was determined. Analysis indicated 2.98 percent carbon after 8 hours' grinding and 4.56 percent carbon after 12 hours' grinding. Additional analyses will be necessary to determine the effectiveness of the vacuum treatment at 300°F for removal of absorbed alcohol.

3. Future Work

Although the cause of the iron and chromium contamination is related to the stainless steel attritor components, previous experience in grinding beryllium to the same particle size range (1 micron) indicated only 1.13 percent iron. This previous work utilized Pechiney flake beryllium as opposed to the QMV powder, and a larger attritor with greater grinding efficiency was used. In view of these results the following work will be performed:

- - - - - - - - - - -

* See section III B for description of handling procedures.

TABLE I

Particle Size and Chemical Analyses of -200 mesh QMV

Beryllium Attrition Ground in Methyl Alcohol

Grinding Time (hrs)	Particle Size (microns)	%Iron	%BeO
0	-74	0.05	0.8
2	-20	2.46	2.5
4	-15	6.25	-
6	-10	8.85	-
8	-8	10.75	-
10	-5	12.35	-
12	-3	13.05	10.8

TABLE II

Chromium Content of Ground Powder

Grinding Time (hrs)	% Chromium
0	<0.01
4	1.62
8	2.84
12	3.40

(1) A larger attritor is being incorporated into expanded dry-box facilities with improved procedures for maintaining good inert atmospheres. It is expected that the increased grinding efficiency will reduce grinding times and therefore iron and oxygen contamination

(2) Since the original particle shape and oxygen content of the beryllium may affect grinding efficiency and contamination, -110 mesh Pechiney beryllium powder has been ordered for grinding studies. It is expected that the lower oxygen content of this material may minimize abrasive action on the stainless steel components of the attritor. If the combined effects of a large attritor and flake beryllium do not materially lessen contamination, beryllium tools will be used in the attritor.

(3) The effectiveness of the vacuum treatment at 300°F to remove residual adsorbed alcohol will be evaluated by carbon analysis of degassed powders after grinding.

(4) The grinding processes will be evaluated with respect to particle size and contamination to select a procedure for preparing wrought beryllium with varying oxide contents.

E. Subcontract No. 10a - Pechiney - A. Saulnier, R. Syre and P. Vachet - Recrystallization and Grain Growth in Beryllium

1. Introduction

The object of the program is to study the distribution of oxide in beryllium sheet of differing metallurgical origin, and to determine the effect of this distribution and impurity level on recrystallization and grain growth. The metal is to have two origins: commercially pure Brush beryllium and Pechiney SR flake. The Brush beryllium has been shipped but has not arrived at Chambrey. Fabrication of the SR grade Pechiney beryllium is in process.

2. Fabrication of Samples from SR Grade Pechiney Beryllium Flake

a. Production of Ingots

Two lots of SR flake (87 and 89) have been used for this fabrication. Chemical analyses of these two lots are shown in Table III.

b. Melting

Three 3-kg billets have been produced by vacuum induction melting of flake in a BeO crucible. Melting took place in a vacuum of 10^{-4} mm of Hg. The melt was poured at 1400°C into a graphite mold in Argon T (Table IV) after holding under Argon T. The billet was then cooled in vacuum. Two mm were skinned from the ingots, which were then radiographed to determine the extent of the shrinkage pipe. The bottom of one ingot (diameter 95 mm, height 120 mm), designated H-1190, has been canned for forging in a half-hard steel, 10 mm thick.

c. Attrition

The top of ingots H-1190 and H-1191 were turned under a blanket of argon into chips 0.10 to 0.15 mm thick. The third ingot was set aside in case of a fabrication accident. The chips were ground in lots of 1-1/2 kg under purified Argon U (see Table IV). Screening was done manually through screens of French sieve sizes 50, 110 and 200. The two size ranges (-50+110 and -200) have been obtained after 24 and 200 hours of grinding respectively. The +50 and +200 fractions remaining were saved.

d. Production of Forging Billets

Three forging billets have been made under the following conditions: 1 billet, diameter 95, height 120 mm, taken from vacuum induction melted SR flake ingot, designated H-1190 SR; 1 billet, diameter 89, height 55 mm, sintered from SR powder, -50+110 mesh, designated A-19-SR; and 1 billet, diameter 88, height 67 mm, sintered from SR powder, -200 mesh, designated A-18-SR.

The analyses of these billets are given in Table V. It may be seen from Table VI that the oxide and metallic impurity content increases during the grinding of the ingot chips, increasing with decreasing average grain size.

The size distribution of the -200 mesh powder has been checked (Table VII) after homogenization under purified Argon U (Table IV) using the usual French screen series.

Sintering was carried out by cold pressing the powder in a solid steel can under a pressure of 100 kg/mm^2 and then by hot pressing at 950°C under a pressure of 100 kg/mm^2. This was followed by removal of the canning material and machining of the billets to maximum dimensions. The sintered billets were then recanned under the same conditions used for the cast billet. The canning consists of a thick half-hard seamless steel tube internally machined to the exact diameter of the beryllium billet, and two covers, also of steel, arc welded to both ends of the tube. The forging operation consisted of pressing the unrestrained canned billets between two preheated anvils. The deformation rate is low and the average reduction is 4:1, corresponding to a reduction in thickness $\left(\frac{100[H-h]}{H}\right)$ of 75 percent. The temperature of the forging was between 780 and 900°C, with the maximum force being 666 tons or a pressure of 22 kg/mm^2. The resulting plates are being machined into rolling slabs approximately 15 mm in thickness. They will be checked by macro examination, radiography and hardness tests. The scrap portions will also be saved for structural examination. The hot rolling operation will be done during the month of July.

TABLE III

Chemical Analysis of Lots 87 and 89, SR grade Pechiney Flake

(in parts per million by weight)

Lot No.	Cr	Ca	Ni	Zn	Cu	Al	Si	Ti	Mg	Mn	Fe	B	Na	BeO	Cl	C
87	<2	30	27	32	<5	<30	10	<2	<10	<2	7	1	150	350	350	140
89	<2	<30	30	20	<5	<30	10	<2	<10	<2	10	1	150	600	465	130

TABLE IV

Analysis of Argon

(parts per million by weight)

	Water Vapor	N_2	O_2
Argon T	12	20	10
Argon U	12	80	3

TABLE V

Spectrographic Analysis of Pechiney SR Beryllium Forging Billets

(in parts per million by weight)

Billet No.	Cr	Ca	Ni	Zn	Cu	Al	Si	Pb	Ti	Mg	Mn	Fe	B	Na	Mo	BeO	Cl	C
H 1190 SR (cast)	<10	50	64	<80	32	<30	35	<15	<25	25	<5	35	1	<100	<15	1200	<20	250
A 19 SR (-50 +110)	12	45	44	<80	5	65	25	<15	<25	36	<5	60	1	<100	<15	2000	<20	250
A 18 SR (- 200)	11	50	50	<80	23	65	75	<15	<25	60	<5	120	1	<100	<15	1.36%	<20	300

TABLE VI

Relationship between Billet Grain Size and Metallic Impurity and BeO Contents.

	Grain Size	Metallic Impurity Content (parts per million by weight)	BeO* %
Cast	.2500	522	0.12
Powder (-50+110)	260	535	0.20
Powder (- 200)	65	695	1.36

*Insoluble in bromine methanol.

TABLE VII

Size Distribution of -200 Mesh Powder

Screen Size	Opening	Percent Passing through Screen
200	80	99
250	63	48
300	50	38
350	42	29
430	35	21

F. Subcontract No. 10b - Pechiney - A. Saulnier, R. Syre and P. Vachet - Identification of Impurities and Precipitates in Beryllium

1. Introduction

The object of this program is to compare the inclusions and precipitates contained in the following materials:

Group 1. Commercially pure Brush beryllium and SR grade Pechiney beryllium (taken from the Recrystallization and Grain Growth Program).

Group 2. Commercially pure Pechiney beryllium, beryllium-iron alloys containing 0.03, 0.1, and 0.25 w/o iron, beryllium-aluminum alloys containing 0.05, and 0.2 w/o aluminum, and beryllium-silicon alloys containing 0.02 w/o silicon, all produced from SR grade Pechiney beryllium.

Group 3. High purity beryllium furnished by Nuclear Metals.

2. Fabrication of Commercially Pure Pechiney Beryllium

Three kg of commercially pure beryllium flake (Lot no. 4) were induction melted and cast under a pressure of argon into an ingot 100 mm in diameter designated H-1168. The ingot was skinned to 95 mm diameter then cut into two parts. The bottom part, approximately 0.8 kg, was canned in soft steel and hot-pressed at 800°C to eliminate any micro-porosity. The top part was turned into chips which were ground under Argon T (Table IV) in a mill with stainless steel balls (ground for 30 minutes after cooling to -15°C). The -110 mesh powder, obtained by screening under argon, was cold pressed into a soft steel can and sintered by hot pressing at 550°C in an 800-ton Loewy press. Analysis was performed on chips from the center of Ingot H-1168 (Table VIII). The cast billet and the sintered billet was extruded in cans in the 800-ton press into flats 55 x 16 mm with a reduction in area of 9:1. The billet temperature was 950°C; container temperature, 430°C; pressure at the start of extrusion, 40 kg/mm^2, and at the finish, 80 kg/mm^2; and the average speed of extrusion, 1.2 meters per minute. The flats were decanned and

TABLE VIII

Chemical Analysis of Induction-Melted Billet
Produced from CR Grade Pechiney Flake

(in parts per million by weight)

Ingot No.	Cr	Ca	Ni	Zn	Cu	Al	Si	Pb	Ti	Mg	Mn	Fe	B	Na	Mo	BeO	Cl	C
H-1168-CR	6	<30	95	<80	48	40	<15	<15	<25	<10	25	195	1	<100	<15	960	-10	220

machined into slabs approximately 100 x 50 x 10 mm and hot rolled in stainless steel cans. The main rolling direction corresponded to the direction of extrusion and the rolling temperature was 800-850°C for the cast metal and 850-900°C for the sintered material. Finish passes were performed under the same conditions after removal of the canning material. The final thickness of the sheets is approximately 1 mm.

3. Production of Master Alloys

As a prelude to the production of beryllium-iron and beryllium-aluminum alloys, two master alloys, beryllium 10 w/o iron and beryllium 1 w/o aluminum, have been produced starting with SR grade flake. The flake was taken from Lot 89 and pressed with either electrolytic iron powder or refined aluminum chips. The alloys were melted in a vacuum of 10^{-4} mm Hg held at 1500°C under a pressure of 60 mm of argon and cast. The ingots were then skinned to a depth of 2 mm into chips 0.3 to 0.4 mm thick. The results of analyses carried out on these chips are given in Table IX. The analysis of the beryllium-aluminum alloy is correct; that of the beryllium - 10 w/o iron alloy shows a contamination in metallic elements arising from either the crucible (aluminum-silicon-calcium) or the quality of the iron used (manganese-nickel-chromium). It is felt that this contamination will be of no consequence to this study since the master alloys will be diluted to produce 0.03, 0.1 and 0.25 w/o iron alloys.

4. Production of Alloys

Alloys have been produced by pressing SR flake (lots 89 and 98) with the required portion of chips from the master alloys. (One exception is the beryllium-silicon alloys, where the addition was made in the form of pure silicon powder). The compression was followed by vacuum fusion (10^{-4} Torr) in a sintered beryllium oxide crucible especially reserved for this fabrication. The melt was maintained for one-half hour under a small pressure of Argon T* (60 Torr) and cast at

- - - - - - - - - - -

* See Table IV for analysis.

TABLE IX

Chemical Analysis of Master Alloys and Starting Materials

(parts per million by weight)

Designation	Cr	Ca	Ni	Zn	Cu	Al	Si	Pb	Ti	Mg	Mn	Fe	B	Na	Mo	BeO	Cl	C
SR Flake Lot No. 89	<2	<30	30	20	<5	<30	10		<2	<10	<2	10	1	150		600	465	130
SR Flake Lot No. 98	<2	<30	18	32	<5	<30	14		<2	<10	<2	6	1	150		500	575	140
H1193-Al	<10	30	42	<80	26	9300	<15	<15	<25	10	<5	35	1	150	<15	1500	<20	300
H1194-Fe	38	250	125	<80	69	220	110	<15	<25	40	210	97200	1	<100	<15	1600	<20	270

1500°C into a nuclear-grade graphite mold.

The six ingots have been cast without difficulty. After skinning to a depth of 2 mm, samples for analysis have been taken from the top and bottom of the ingot. Chemical analysis of the additive element has shown that the contents obtained were close to those envisioned except for the beryllium-silicon alloy, which is due to be remelted under the same conditions to improve its homogeneity. The complete analytical results (with the exception of carbon) are reported in Table X. A slight heterogeneity of Alloy H-1230 has been noted in the 0.03 w/o aluminum alloy. Also, the anomalous silicon content of this alloy will be checked.

The ingots have been radiographed using the usual techniques employed at Pechiney (41 Kv, 5 milliamps, 2 minutes at 110 cm from Kodak M film). The transparency of the metal appears to vary directly with the content of iron. The bottoms of the ingots are perfectly sound with neither inclusions nor visible cracks, up to a height determined by the depth of the shrinkage cavity. For the alloy containing 0.25 w/o Fe, designated H-1226, the height is 115 mm; for the Be - 0.10 w/o Fe alloy, H-1227, the height is 80 mm; for the Be - 0.003 w/o Fe alloy, H-1228, the height is 80 mm. For the Be - 0.20 w/o Al alloy, H-1229, the height is 120 mm; for the Be - 0.05 w/o Al alloy, H-1230, the height is 55 mm.

5. Fabrication of Alloys

The five alloys previously mentioned were fabricated by extrusion and hot rolling. The steps in this process consisted of canning in soft steel 2 mm thick, hot pressing in a can after preheating in argon (850°C at 100 kg/mm^2). This operation is intended to eliminate microcracks not detectable by radiography. Hot pressing was followed by extrusion of the canned billets into a flat after preheating in argon at 950°C. An extrusion reduction of 9-1/2:1 was used. The extrusion variables are summarized in Table XI. After extrusion, the flats were machined into bars 60 x 50 mm, canned in thin stainless steel and welded for hot rolling. The rolling of these five alloys and the

TABLE X

Analysis of Beryllium Alloy Ingots

(in parts per million by weight)

Ingot No.	Sample Position	Cr	Ca	Ni*	Zn	Cu	Al*	Si	Ti	Mg	Mn	Fe*	Na	BeO**	Cl*
H-1226 (Be-Fe)	top	<10	<30	<25	<80	<5	<30	15	<25	<10	<5	2500	<100	1800	20
	bottom	<10	<30	<25	<80	<5	<30	<15	<25	<10	<5	2400	200	2000	<20
H-1227 (Be-Fe)	top	<10	<30	<25	<80	<5	<30	20	<25	<10	<5	1050	<100	2300	<20
	bottom	11	30	25	<80	<5	<30	30	<25	12	<5	1150	<100	2600	<20
H-1228 (Be-Fe)	top	<10	<30	< 5	<80	<3	30	<15	<25	<10	<5	500	<100	2600	<20
	bottom	<10	<30	<25	80	<3	30	<15	<25	<10	<5	500	<100	2000	<20
H-1229 (Be-Al)	top	<10	<30	<25	<80	6	2200	30	<25	<10	<5	30	100	1800	<20
	bottom	<10	<30	<25	<80	<5	2100	<15	<25	<10	<5	35	130	2000	<20
H-1230 (Be-Al)	top	<10	<30	<25	<80	<5	300	20	<25	10	<5	45	100	1400	<20
	bottom	<10	<30	<25	<80	5	500	220(?)	<25	<10	<5	40	<100	1600	<20

* Chemical analysis. Other elements analyzed spectrographically.

** Insolube in bromine methanol. This technique gives high results.

TABLE XI

Variables in the Extrusion of Beryllium Alloys

Alloy (w/o)	Ingot No.	Extrusion Pressure (kg/mm^2) (start)	(finish)	Maximum Speed (m/min.)	Appearance
Be-Fe 0.25	H-1226	60	90	5.3	good
Be-Fe 0.10	H-1227	67	100	16	good
Be-Fe 0.03	H-1228	63	93	5.3	good
Be-Al 0.20	H-1229	35	74	3.9	crack
Be-Al 0.05	H-1230	35	70	5.3	good

extrusion of the beryllium-silicon alloy will be done during July. Plans have been made for the fabrication of powder (-110 mesh) made from two alloys having the larger alloy additions, beryllium 0.25 w/o iron and beryllium 0.20 w/o aluminum. The grinding of chips is now under way.

6. Metallographic Studies

a. Preliminary Studies

While waiting for the production and fabrication of samples, a few preliminary studies have been made on alloys outside of the program.

A method has been developed which permits the obtaining of thin films from samples as thick as 0.8 mm. These samples are directly observable in the electron microscope without the introduction of parasitic strains. The procedure consists of an initial chemical thinning in a solution of 20% nitric acid, 10% hydrofluoric acid and water. The thickness is reduced from 0.8 to 0.05-0.06 mm. This is then followed by an electrolytic thinning by the usual method used at Pechiney: a Disa-electropol is used with the E2 bath at 45 volts for approximately 10 seconds.

Some preliminary studies have been conducted on the metallographic preparation of a sample of beryllium which had been cast, extruded and rolled. The technique applied an etching method used by Meredith and Sawkill[23] using the A2 solution of the Disa-electropol, which was purposely contaminated with copper. The etching effectively revealed the substructure and perhaps the impurities (Fig. 5). The features observed were found to vary as a function of thermal treatment, but the relationship between the etched structure and the structure observed by electron metallography of thin films produced from similar samples (Fig. 6) is difficult to establish with certainty. In particular, it is very rare to find inclusions in the thin samples.

A few examinations have been attempted on thin metallic samples of Be - 0.2 w/o Al alloy in the cast and extruded state. In this

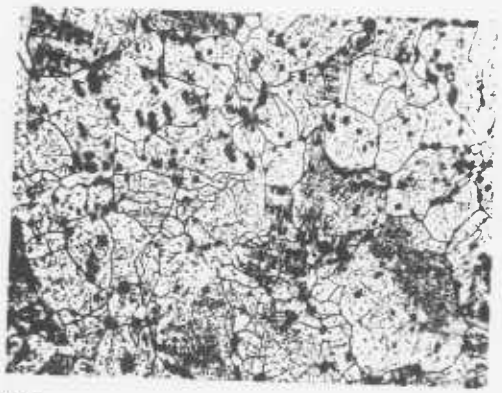

265X

Fig. 5 - Beryllium cast, extruded and rolled to 0.07 mm. Polished in A? electrolyte containing copper. The microstructure is revealed by a deposit of copper.

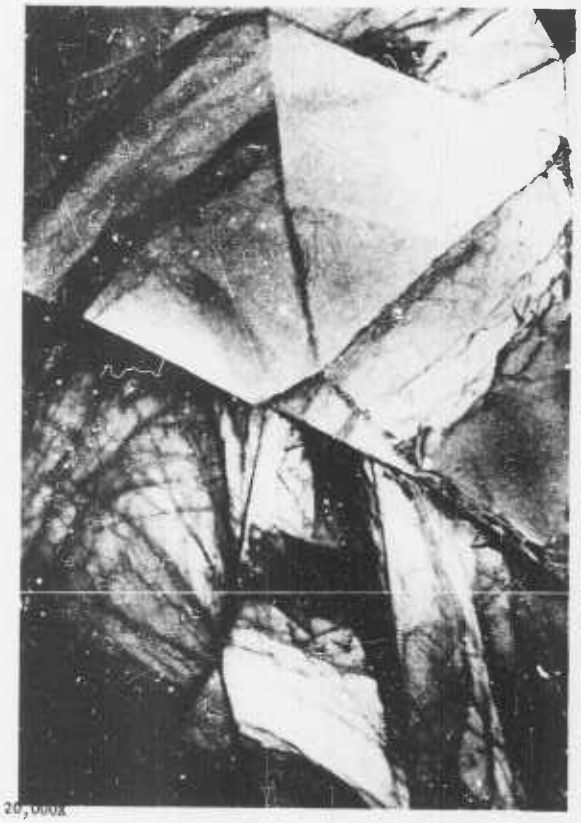

20,000X

Fig. 6 - Cast beryllium extruded and rolled to 0.05 mm.

examination it has been possible to identify certain intergranular inclusions by electron micro-diffraction. Figure 7 shows one such constituent and its electron diffraction pattern, which corresponds to none other than the (112) plane of the reciprocal lattice of aluminum. The characteristics of one of the many such constituents have been investigated (Fig. 8). In heating the sample inside the microscope with the aid of a Siemens micro-furnace it has been possible to observe the movement of these constituents into the grain boundaries at elevated temperature.

The successive changes in one of these constituents is represented in Fig. 8. At approximately 400°C, the particle begins to extend along the grain boundary; towards 500°C the phenomenon is accentuated and, if heating is continued, complete fusion is produced and the liquid penetrates deep into the boundary (Fig. 8d). Although the temperature cannot be measured precisely, it is practically certain that this melting begins at a temperature considerably lower than the melting point of aluminum. It is therefore probable that aluminum has dissolved one or more impurities which lower its melting point and/or changes its surface energies.

b. Photographic Examination of Commercially Pure Beryllium in the Cast, Cast and Extruded, and Cast, Extruded and Rolled States

A summary of the results obtained thus far is presented below:

(1) Cast State

(a) Optical Micrography. Several inclusions and a large amount of porosity were found. (Fig. 9)

(b) Electron Microscopy Extraction Replicas. Particles of beryllium oxide (Figs. 10 and 11) have been found, as well as a number of other crystals which have not been identified up to the present (see example in Figs. 12 and 13).

0.1 μ

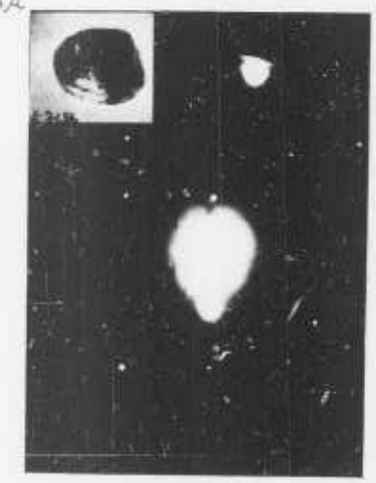

Fig. 7 - Be - 0.2 w/o Al alloy cast and extruded. (112) of Al.

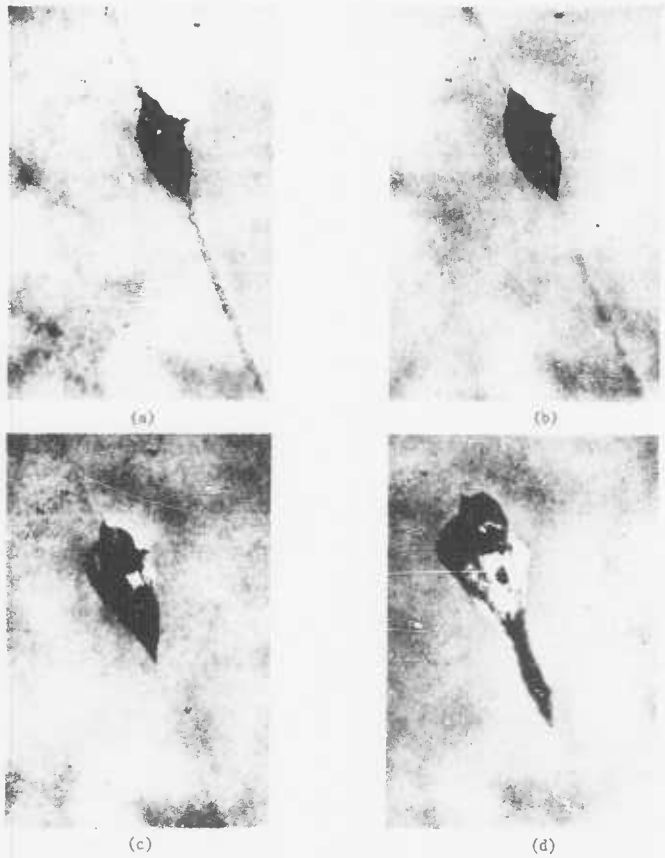

Fig. 8 - Be - 0.2 w/o Al alloy cast and extruded. (a) as extruded (b) heated to 400°C, (c) heated to 500°C, (d) heated to 550°C 10,000 X. 1 μ

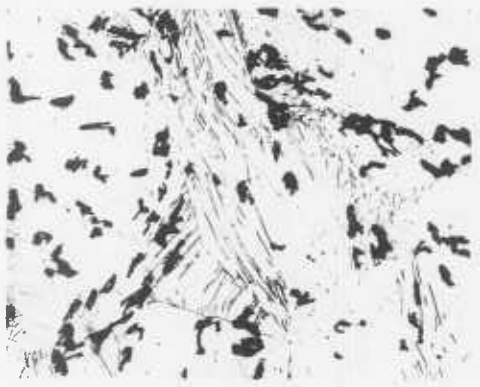

Fig. 9 - Cast metal produced from CR grade Pechiney flake. Optical micrograph showing porosity. 130X

Fig. 10 - Cast metal extraction replica, BeO. 50,000X

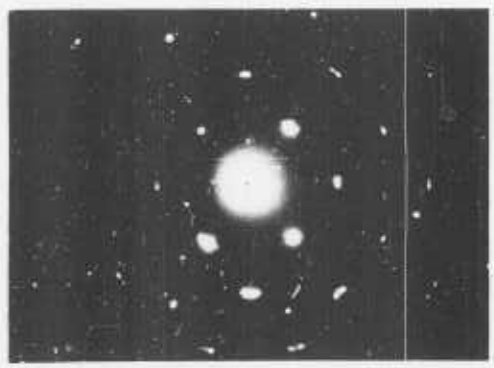

Fig. 11 - Microdiffraction pattern corresponding to Fig. 10. BeO (1101) reciprocal lattice plane.

Fig. 12 - Cast metal extraction replica. 40,000X

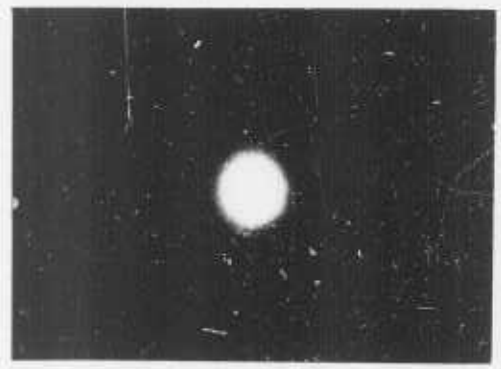

Fig. 13 - Microdiffraction pattern corresponding to Fig. 12. Rings at 3.33, 2, 1.21, 1.14 and 1.04 Å.

(2) Cast and Extruded State

(a) Optical Microscopy. The presence of fine inclusions was revealed. (Fig. 14)

(b) Electron Microscopy Extraction Replicas (double-replica celluloid and carbon). Figure 15 shows an inclusion found in this material. The corresponding electron diffraction pattern is poor and difficult to interpret. It is probably BeO.

(c) Electron Microscopy Thin-Film Technique. These samples have been taken either parallel or perpendicular to the extrusion direction. (Figs. 16-20) They show dislocations and impurities.

The particles observed diffract poorly. Perhaps the preparations are themselves too thick, so that multiple diffraction occurs in the matrix of beryllium as evidenced by the Kikuchi lines that are observed. Perhaps, also, the inclusions are themselves very large and opaque to electrons. Attempts are being made to resolve these difficulties.

(3) Samples Cast, Extruded and Rolled to 1 mm Thickness

(a) Optical Microscopy. The grains are rather large and some inclusions have been noted. (Fig. 21)

(b) Electron Microscopy Extraction Replica (direct carbon replica). The inclusions are very easily extracted and in most cases are BeO, as is shown in Figs. 22 and 23.

(c) Thin-Film Electron Microscopy. (Figs 24-27) The micrographs taken of thin films show the images of the dislocation networks. They also permit the isolation of inclusions and the attempt at identification by electron microdiffraction. Particles of BeO and Si have thus been identified; however, the identification of silicon requires further confirmation. The microdiffraction patterns are generally very poor and the major part of our effort in performing this work will consist in improving the diffraction technique.

Fig. 14 - Cast and extruded state. Optical micrograph of a longitudinal section showing fine inclusions. 130X

Fig. 15 - Cast and extruded state. Particle obtained by extraction replica technique. 40,000X

Fig. 16 - Dislocations in cast and extruded metal. Film thinned parallel to the extrusion direction. 20,000X

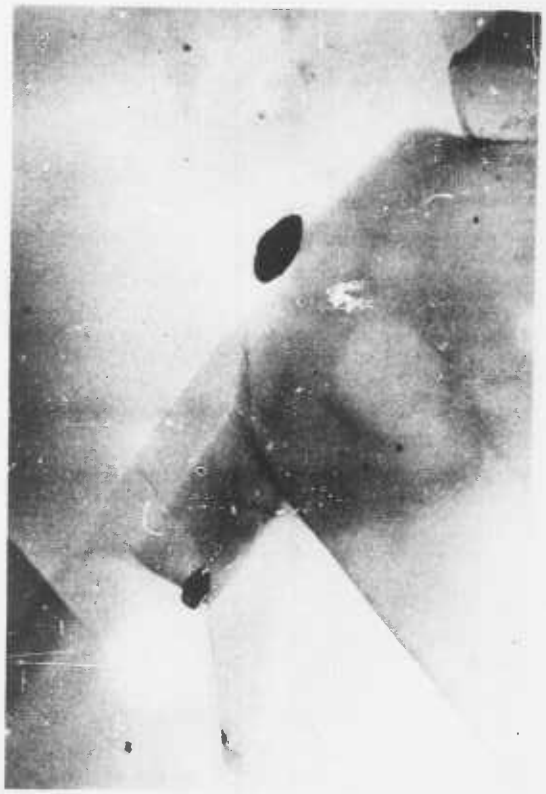

Fig. 17 - Inclusions in cast and extruded metal. Film thinned parallel to extrusion direction. 20,000X

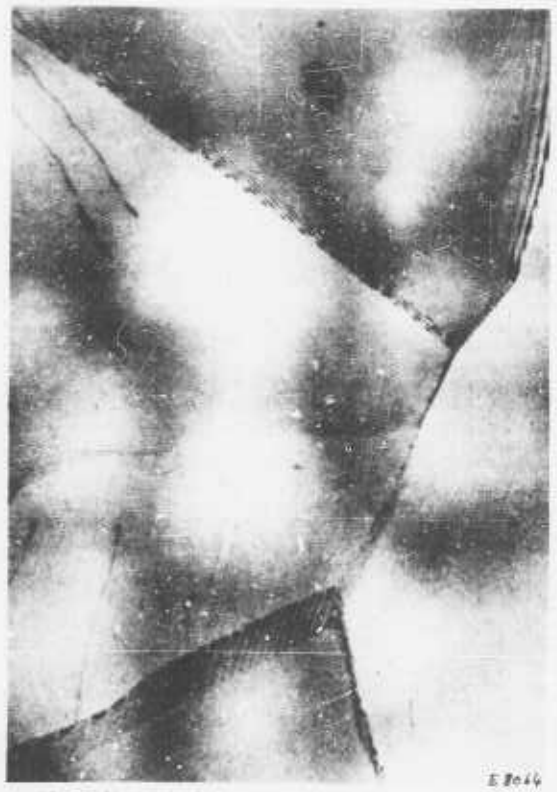

Fig. 18 - Walls of dislocations present in cast and extruded metal thinned parallel to the extrusion direction. 20,000X

Fig. 19 - Dislocation pattern in cast and extruded metal thinned perpendicular to the extrusion direction. Diffraction pattern corresponds to the (1101) reciprocal lattice plane. 50,000X

Fig. 20 - Inclusion in cast and extruded metal thinned perpendicular to the extrusion direction. Diffraction pattern shows a spot at 3.74 Å and the (1100) reciprocal lattice plane of Be. 50,000X

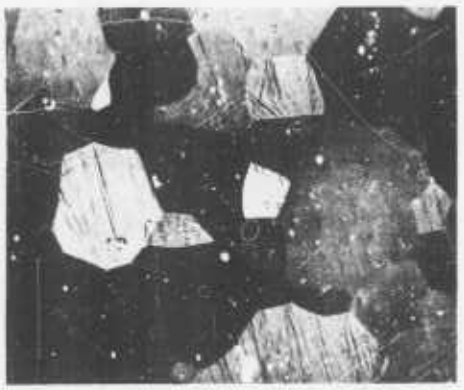

Fig. 21 - Recrystallized grains and inclusions in cast, extruded and rolled metal (1 mm thickness). Optical microscopy. 130X

E8043

Fig. 22 - Inclusion of BeO in extraction replica of cast, extruded and rolled metal (rolled to 1 mm thickness). 40,000X

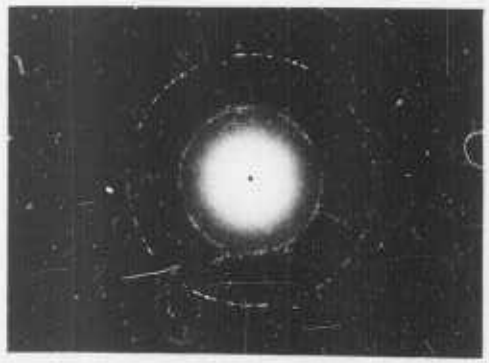

Fig. 23 - Electron microdiffraction pattern corresponding to Fig. 22. BeO.

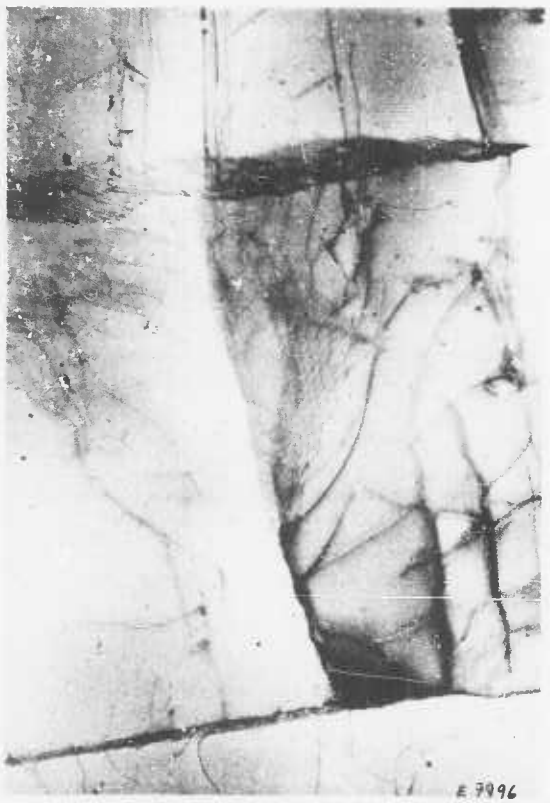

Fig. 24 - Transmission electron micrograph. Networks and walls of dislocations in cast, extruded and rolled Be. 50,000X

Fig. 25 - Inclusions, tentatively identified as Si, present in a thin film of cast, extruded and rolled Be. 50,000X

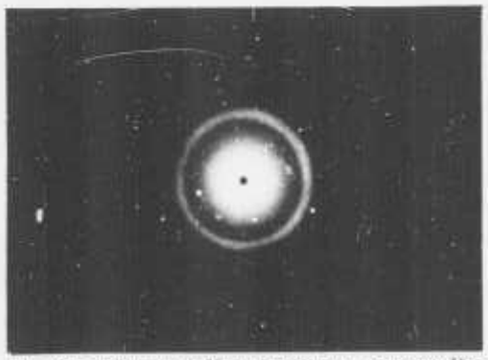

Fig. 26 - Electron diffraction pattern corresponding to Fig. 25, showing rings of BeO and (001) Si.

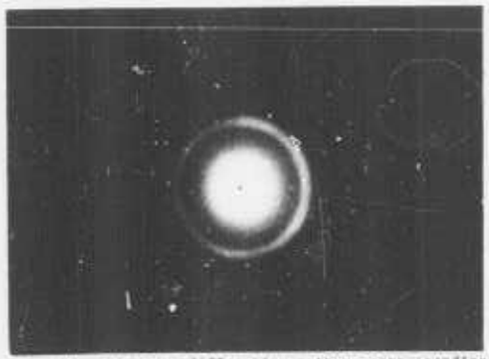

Fig. 27 - Electron diffraction pattern corresponding to Fig. 25 after rotation of the sample, showing BeO rings and Si spots.

c. Metal of High Purity

(1) Initial Samples (received the 7th of May from Nuclear Metals, Inc.). This first shipment consisted of samples of such small dimensions that they have been very difficult to thin. However, two electron micrographs have been obtained on Sample No. 6 (distilled and zone-refined beryllium crystal, 5 passes, specimen taken from near last region to solidify, designated crystal ZR-7C). Some observations have been made by optical microscopy.

Sample No. 1, vacuum-melted Pechiney flake CR grade: some widely dispersed polygonal inclusions.

Sample No. 3, double-distilled beryllium, distillate No. 26: large grains, few inclusions.

Sample No. 4, distilled, vacuum-melted and extruded: very fine grains, few inclusions.

Sample No. 6, distilled and purified by zone-refining, 5 passes, specimen taken from near last region to solidify: a few small inclusions.

(2) Second Shipment of Samples from Nuclear Metals. Two samples were received on June 26 and are being examined.

III. PROJECTS AT NUCLEAR METALS, INC.

A. Preparation and Evaluation of High Purity Beryllium - E. D. Levine and J. P. Pemsler.

1. Summary

During the present quarter, efforts were directed toward the preparation of double-distilled beryllium for mechanical property evaluation and the evaluation of material of various purity levels prepared by powder metallurgy techniques.

2. Preparation of Double-Distilled Beryllium

Measurements of resistance ratios and observations of fracture surfaces, reported previously,[1] indicated that double-distilled beryllium may contain a significantly smaller amount of both

soluble and insoluble impurities than single-distilled beryllium. Extensive experiments for the mechanical evaluation of double-distilled beryllium have therefore been planned.

During the third quarter, three cones of double-distilled berryllium, comprising a total of ~1000 grams, were prepared. Each re-distillation was performed on two single-distilled cones which had been consolidated by vacuum melting in the distillation apparatus. Since resistance ratio measurements[1] indicated that an impurity gradient exists in single-distilled deposits, the impurity content increasing toward the cooler region near the top of the cone, the upper one-third of each single-distilled cone was cropped off prior to consolidation for re-distillation.

A portion of the double-distilled material will be subjected to further purification by zone refining prior to evaluation. The remainder will be consolidated to a reasonably fine-grained bulk form for evaluation.

3. Evaluation of High Purity Beryllium by Powder Metallurgy Techniques

One of the difficulties in evaluating the mechanical properties of distilled beryllium is obtaining test samples of suitable metallurgical quality. The large grain size and porosity of as-deposited material necessitates the use of consolidation procedures that produce densification and permit some control over grain size and orientation texture, while maintaining the high purity characteristic of the as-deposited material. Previous attempts to fabricate distilled material by vacuum melting, extrusion and rolling[27] were only partially successful in controlling the above variables.

In order to aid in the selection of fabrication procedures for consolidation of double-distilled beryllium, experiments have been initiated to evaluate material of various purity levels by powder metallurgy techniques. The following materials, listed in order of increasing purity, are being studied:

(1) Brush QMV -200 mesh powder
(2) Vacuum-melted CR grade Pechiney flake
(3) SR grade -110 mesh powder
(4) 5-pass zone-refined CR grade Pechiney flake
(5) Single-distilled beryllium
(6) Double-distilled beryllium

Fifty-gram batches of vacuum-melted Pechiney flake, zone-refined beryllium, and single- and double-distilled beryllium were attritioned in a mortar and pestle fabricated from CR grade beryllium. Since previous experience[27] had shown that severe contamination of distilled powder occurs during sizing operations, the powders prepared in the present experiments were not sized. The average particle size of these powders was approximately 200 microns. The largest particles were approximately 500 microns.

Chemical analyses of powder prepared from single- and double-distilled beryllium, shown in Table XII, revealed little contamination except for a small amount of iron pickup, probably from dust particles in the atmosphere.

Powder from each of the above batches was cold compacted in a beryllium die at 10 tons/in.^{2} and sealed in 1-inch inside diameter outgassed steel cans. The billets were extruded at 1650°F into flats having a cross-section of 3/4 x 0.075 inch.

The extruded flat prepared from single-distilled powder had an elongated blister over its entire length, and the cross-section contained numerous voids. No mechanical test specimens could be obtained from this extrusion. The other extrusions, however, were successful, and are presently being machined into tensile and bend specimens.

4. Oxygen Content of Distilled Beryllium

Samples of single-distilled beryllium and vacuum-melted Pechiney flake, prepared at Nuclear Metals, Inc., have been analyzed for oxygen by a fast neutron activation technique by R. F. Coleman,

TABLE XII

Chemical Analyses of Powders Attritioned from Single- and Double-Distilled Beryllium

(in parts per million by weight)

	Single-Distilled		Double-Distilled	
Impurity	Sample 1	Sample 2	Sample 1	Sample 2
Fe	25	9	6	9
Si	24		13	
Cr	2		<1	

of the Atomic Weapons Research Establishment, Great Britain. The results are presented in Table XIII. They indicate that distillation, under the conditions employed at Nuclear Metals, Inc., does not remove oxygen, but that vacuum melting reduces the oxygen content somewhat. It is hoped that additional analyses will be performed by neutron activation and other techniques during the present program

5. Future Work

In the next quarter, it is planned to complete the evaluation of the meterial prepared by powder metallurgy techniques. Procedures for consolidating double-distilled beryllium will be determined upon the analysis of the above evaluation.

B. Fabrication and Evaluation of Fine-Grained Beryllium Produced From Ultra-Fine Powders - A. K. Wolff

1. Summary

During the past quarter, work has proceeded on the construction of an inert atmosphere pressing apparatus for packing of ultra-fine beryllium powders being prepared at New England Materials Laboratory and National Research Corporation. In addition, chemical evaluation has been made of some preliminary grinding experiments carried out at NEM Lab.

2. Construction of Pressing Facility

An inert atmosphere pressing facility having a 150-ton capacity has been designed and constructed at Nuclear Metals, Inc. and is in the final stages of assembly and checkout. A schematic drawing (Fig. 28) illustrates the setup. The 150-ton capacity Rodgers hydraulic cylinder is located outside of the glove box both to conserve space and to eliminate possible contamination by the hydraulic fluid. The hydraulic pressure is supplied by an electrically operated Vanguard pump and is transmitted into the box by means of a hardened steel cylinder operating

TABLE XIII

Oxygen Content of Beryllium by Fast Neutron Activation Analysis

Specimen	Oxygen, ppm
Vacuum-Melted Pechiney Beryllium	55
Distilled Beryllium, Distillate No. 17	90-140
Vacuum-Melted Distilled Beryllium	65- 90

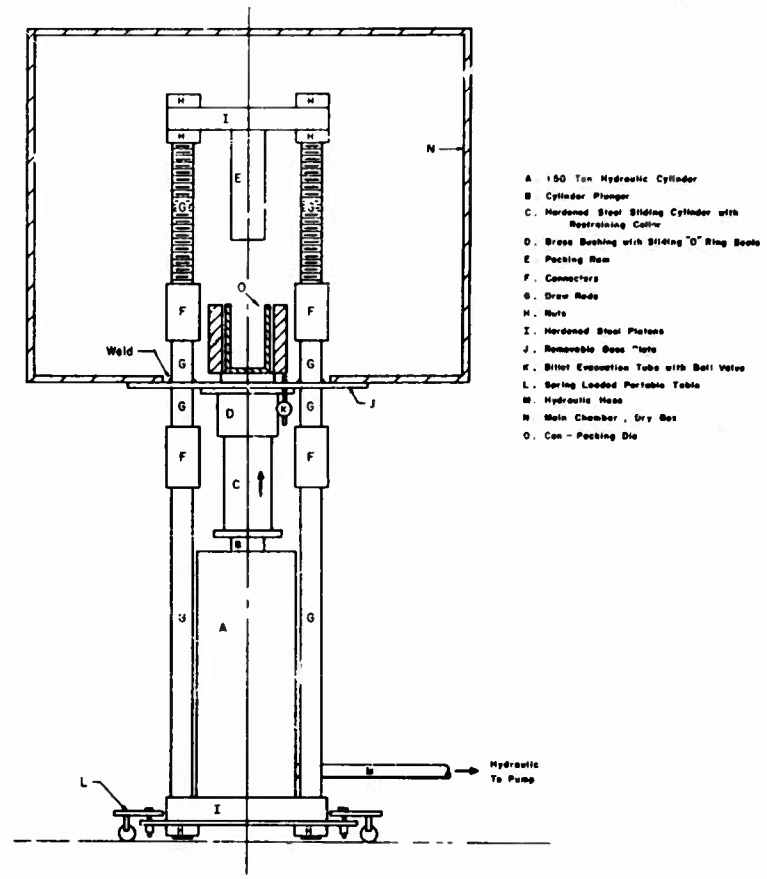

Fig. 28 - Schemetic of inert atmosphere pressing facility.
RA 2366

through a series of "O" ring seals. A collar, held by set screws, is attached to the cylinder to prevent its being drawn into the box during evacuation. The four drawrods (only 2 are shown in the schematic, to avoid confusion) are welded through the glove box base plate. A prior study of weld compatibility and tensile strength demonstrated that there was no significant loss of drawrod properties due to welding. The rods are coupled both above and below the base plate to permit rapid assembly and disassembly of the system. Since the pressing system is self-contained, no significant stresses are placed on the glove box during the pressing operation. A spring-loaded, caster-supported table permits portability of the 270-pound cylinder and allows for elastic expansion of the system during pressing. An evacuation tube, closed with a 1/4-inch ball valve, is also located in the base plate. This will permit the evacuation of the billets.

The entire system has been installed and leak tested. A vacuum of less than 10 microns can be readily obtained in the main chamber.

Rams and billet cans are presently being machined, and standard QMV powder will be used to check out pressing capacity and packing procedure.

3. Chemical Evaluation of Preliminary NEM Lab Grinding Experiments

Oxygen and iron analyses were originally obtained for Brush QMV powders which had been ground at NEM Lab with stainless steel balls for times up to 12 hours. Chloride volatilization was employed for oxygen analysis, and colorimetric methods to determine the iron content.

Samples for oxygen analysis, in the form of small hydrostatically compacted pellets, were transferred to Nuclear Metals, Inc. under inert atmosphere. Each sample container was opened in the dry-box under a purified helium atmosphere and the pellet transferred to a platinum boat. The boat was then sealed in the oxygen analysis reaction vessel, which was removed from the glove box and placed into the chloride

generation system. The system was carefully flushed with argon before the valves of the sealed reaction vessel were opened, ensuring that no contamination would occur during the early stages of acid generation. Slow heating of the system was originally used to prevent a possible reaction between the beryllium and residual grinding volatiles. However, the condensation of beryllium chloride caused varying degrees of blockage of the system, and in subsequent analyses the more conventional rapid heating was employed without any observable reaction of the volatiles.

Since the iron analysis involves dissolution in dilute HCl, it was felt that samples slowly exposed to air would be the safest and easiest to handle. Each sample was exposed in a helium atmosphere which was then evacuated to 50 microns. Air was bled into the system in small increments and the sample watched after each increment to ensure that no burning occurred. When atmospheric pressure was reached, the sample could be removed from the dry-box without incident and the subsequent analysis carried out using standard colorimetric techniques.

These same samples were eventually also employed for chromium and carbon analyses in order to determine if the stainless steel balls were contaminating the powder and if room temperature volatilization of the grinding fluid was adequate. Chromium content was determined colorimetrically using S-diphenylcarbazid as reagent, and the carbon content by Leco conductometric analysis.

Results of all analyses may be found in Section IID of this report.

4. Future Work

A careful study of the cold pressing procedures is being carried out using non-pyrophoric QMV powder. This "pilot" test will include cold pressing of the powders, welding, and evacuation of the billet. When this is completed, fabrication of ultra-fine powders from NEM Lab and NRC can be initiated. Analysis of impurity content will be continued for pertinent stages in the preparation of ultra-fine

powders. No conclusive tests have yet demonstrated the pyrophoricity of beryllium powder received to date, and such a test will be made shortly.

IV. REFERENCES

1. Quarterly Progress Report to Aeronautical Systems Division for the Period Janualy 1, 1962 through March 31, 1962, NMI-9519, June 25, 1962.
2. Monthly Progress Report to Aeronautical Systems Division for the Period April 1, 1962 through April 30, 1962, NMI-9520, June 20, 1962.
3. Quarterly Progress Report to Aeronautical Systems Division for the Period September 1, 1961 through December 31, 1961, NMI-9517, April 16, 1962.
4. A. N. Stroh, Advances in Physics 6 (1957) 418.
5. N. J. Petch, Phil. Mag. 1 (1956) 186.
6. A. N. Stroh, Phil. Mag. 3 (1958) 597.
7. J. J. Gilman, Fracture, p. 51, John Wiley, New York, 1959.
8. B. Allen and A. Moore, "The Tough-Brittle Transition in Beryllium", Conference on Physical Metallurgy of Beryllium. London, Oct. 1961.
9. A. H. Cottrell, Trans. AIME 212 (1958) 192.
10. J. D. Eshelby, F. C. Frank, and F R. N. Nabarro, Phil. Mag. 42 (1951) 351.
11. J. S. Koehler, Phys. Rev. 85 (1952) 480.
12. D. W. White and S. E. Burke, "The Metal Beryllium", ASM, Cleveland, Ohio, 1955.
13. N. J. Petch, Prog. Met. Phys., 5 (1954) 1.
14. C. Zener and J. Hollomon, Trans. ASM 33 (1944) 212.
15. A. R. Kaufmann, P. Gordon, and D. W. Lillie, Trans. ASM 42, (1950) 785.
16. A. J. Martin and G. C. Ellis, "The Ductility Problem in Beryllium", Conference on Physical Metallurgy of Beryllium. London, Oct. 1961.
17. R. F. Bunshah, "A Fresh Look at Problems in Beryllium Metallurgy", ibid.
18. A. P. Green and J. Sawkill, J. Nuclear Materials 3 (1961) 101.
19. W. W. Beaver and K. G. Wikle, Trans. AIME 200 (1954) 559.

20. A. B. Brown, F. Morrow, and A. J. Martin, J. Less Common Metals 3 (1961) 62.

21. J. E. Bunce and R. E. Evans, "A Study of the Effect of Grain Size, Texture, and Annealing Treatment on the Properties of Wrought Beryllium Ingot", Conference on Physical Metallurgy of Beryllium, London, Oct. 1961.

22. P. Cotterill, R. E. Goosey, and A. J. Martin, "An Evaluation of the Hydrogen Content of Commercially Pure Beryllium and its Effect on the Ductile-to-Brittle Transition Temperature", ibid.

23. J. E. Meredith and J. Sawkill, "A Precipitation Reaction in Commercially Pure Beryllium", ibid.

24. J. C. Guest and M. J. Hudson, "Tensile Properties of Hot-Extruded Beryllium Rod and Tubing", ibid.

25. C. C. Olds, et al, "High Temperature Ductility of Powder Fabricated Beryllium at High and Low Strain Rates", ibid.

26. A. K. Wolff, S. H. Gelles, and L. R. Aronin, "Impurity Effects in Commercially Pure Beryllium", ibid.

27. Final Report to Aeronautical Systems Division for the Period April 1, 1960 to September 30, 1961, NMI-9516 (ASD-TDR-62-509, Vol. II, in press).

44

END